HIERARCHICAL COMPRESSED SUBSPACE CLUSTERING OF INFRARED SINGLE-PIXEL MEASUREMENTS

Miguel Marquez, Jonathan Monsalve, Kevin Arias, Karen Sanchez, Carlos Hinojosa, and Henry Arguello.

Universidad Industrial de Santander, Bucaramanga, Colombia.

ABSTRACT

Compressive spectral imaging (CSI) acquires coded projections of a spectral scene reducing storage costs. The single-pixel camera architecture (SPC) excels among several CSI devices due to its low implementation cost. Traditionally, before applying any post-processing task, e.g., clustering, it is required to solve a computationally expensive optimization problem to reconstruct the 3D information. Instead, this paper proposes a hierarchical approach to design the sensing matrix of the SPC, such that the pixel clustering task can be performed directly using the compressed infrared SPC measurements without a previous reconstruction step. Specifically, a sensing matrix is designed to extract features directly from the compressed measurements at each hierarchy step. Then, a final segmentation map is obtained through majority voting in the partial clustering results. Through simulations and experimental proof-of-concept implementation, we demonstrate the efficient proposed alternative to estimate clustering maps without relying on oversampling sensing protocols.

***Index Terms*—** Compressive Spectral Imaging, Subspace Clustering, Infrared, Single-pixel Camera.

1. INTRODUCTION

Spectral imaging (SI) acquires two-dimensional spatial information of a scene across a range of spectral wavelengths. Compared to traditional RGB imaging systems, SI provides more detailed information about the pixels in the scene to spectral level, which allows the identification of several target features [1]. In this sense, SI has emerged as a valuable tool for multiple applications, including remote sensing classification, where the goal is to assign a class or label to each pixel of an image [2]. This classification task can be performed by a supervised or unsupervised approach. Supervised approaches require labeled data for a costly training stage to learn the classes' characteristics; in contrast, unsupervised methods assign the classes by discovering hidden patterns in grouping similar pixels. In particular, spectral clustering is an unsupervised technique that has been successfully employed in SI classification when the labeled samples are unavailable or difficult to acquire [3, 4, 5]. On the other hand, the classification task usually improves as the number of spectral bands increases [6]. However, this requires sensing more information, which makes spectral data acquisition and processing challenging under traditional scanning-based methods.

Recently, compressive spectral imaging (CSI) has emerged as a SI approach that acquires compressed projections of the whole data cube instead of directly measuring all the voxels [7, 8]. CSI allows to detect and reduce the dimensionality of the scene in a single step. Consequently, the cost of sensing, storage, transmission, and processing spectral images using CSI devices is significantly reduced [9]. Optimization algorithms that solve the underlying ill-posed problem have been employed to recover the spectral image from the compressed measurements. For instance, the fast iterative shrinkage-thresholding algorithm (FISTA) [10], the gradient projection for sparse representation (GPSR) [11], or the orthogonal matching pursuit (OMP) [12] are state-of-the-art recovery algorithms. Although these optimization algorithms provide good performance, they are computationally expensive and time-consuming. Several works in CSI have focused on designing coding patterns to improve the results of the reconstruction, using side information from a second sensor [13, 14]. However, traditionally the scenes are acquired inside the visible spectrum range, i.e., beginning at 400 nm.

This paper develops an image detection protocol to obtain unsupervised pixel classification directly from the compressive infrared single-pixel camera (SPC) domain (0.9-2.5 um). A hierarchical approach is introduced to design the downsampling matrices preserving the cluster features in a reduced set of compressed measurements. Specifically, the downsampling matrices are generated following a regular size pixels decimation approach, where the pixel size proportionally decreases in function of the hierarchical step. Note that, for each hierarchical iteration, our method estimates a clustering map. Then, we use a majority voting technique among all the estimated maps to build the final segmentation map.

Contribution. In this work, we propose a hierarchical approach to design a sensing matrix of the SPC [15] such that clustering features are extracted directly from the acquired compressed measurements. Specifically, at each level of the hierarchy, we design the sensing matrix as the product of a Hadamard and decimation matrices. Our design allows obtaining a set of features directly from the compressed measurements exploiting the properties of the Hadamard matrix.

In the proposed approach, the decimation matrix at a given level is designed to group more similar spatial features than the previous level. Therefore, the composite sensing matrix has more sampling vectors and it is intended to provide more features than those obtained in the previous level. Lastly, the final segmentation map is obtained by performing majority voting on the partial clustering results obtained using the set of features of each hierarchy level.

2. CSI ACQUISITION SYSTEM

In this paper, the proposed CSI clustering approach is performed on the SPC compressed measurements. The objective lens focuses the input 3D scene $\boldsymbol{\mathcal{F}}$, with L spectral bands and $M \times N$ spatial pixels, onto the coded aperture $\mathbf{T} \in \mathbb{R}^{M\times N}$, that spatially modulates each spectral pixel. The coded aperture $\mathbf{T}$ can be modeled as a binary pattern $\{-1, 1\}$, that blocks the light or lets it pass through each pixel.

2.1. Discrete Sensing Model

Mathematically, the discrete sensing process can be expressed as

$$\mathbf{Y} = \mathbf{H}\hat{\mathbf{F}} + \boldsymbol{\epsilon}, \tag{1}$$

where $\mathbf{Y} \in \mathbb{R}^{K\times L}$ is the compressed measurements acquired in K shots, $\mathbf{H} \in \mathbb{R}^{K\times MN}$ is the coded aperture with $\mathbf{H} \in \{1, 0, -1\}$, $\hat{\mathbf{F}} \in \mathbb{R}^{MN\times L}$ is the matrix form of the 3D datacube $\mathbf{F} \in \mathbb{R}^{M\times N\times L}$, and $\boldsymbol{\epsilon} \in \mathbb{R}^{K\times L}$ represents the additive noise. In order to capture K measurement shots, a different coded aperture pattern is employed each time. The compression ratio in this model is given by $\gamma = \frac{K}{MN}$, where $\gamma \in [0, 1]$.

2.2. Sensing Matrix Design

In general, it is required to solve a computationally expensive optimization problem to recover the underlying spectral scene from the compressed measurements acquired in Eq. 1. Taking into account the structure of Hadamard matrices, [16] proposes to design the sensing matrix for each band $\mathbf{H}$ as

$$\mathbf{H} = \mathbf{W}\boldsymbol{\Delta}, \tag{2}$$

where $\mathbf{W} \in \{-1, 1\}^{K\times K}$ is a Hadamard matrix, and $\boldsymbol{\Delta} \in \mathbb{R}^{K\times MN}$ is a decimation matrix.

Recently, a fast spectral image recovery method was introduced in [17], where authors proposed to design $\boldsymbol{\Delta}$ by obtaining superpixels from an RGB image which was acquired as side information. Specifically, the method named *FMR* [18] takes advantages of the fact that the inverse of a Hadamard matrix is its transposes and perform a fast low-resolution reconstruction for each spectral band as

$$\tilde{\mathbf{f}}_l = (1/K)\boldsymbol{\Delta}^T\mathbf{W}^T\mathbf{y}_l = (1/K)\boldsymbol{\Delta}^T\mathbf{W}^T\mathbf{W}\boldsymbol{\Delta}\mathbf{f}_l \approx \mathbf{f}_l. \tag{3}$$

Note that, instead of performing the complete reconstruction, it is possible to directly extract features from the compressed measurements. In particular, features from the l-th band can be obtained as

$$\bar{\mathbf{f}}_l = \mathbf{W}^T\mathbf{y}_l = \boldsymbol{\Delta}\mathbf{f}_l, \tag{4}$$

where $\bar{\mathbf{f}}_l$ contains the average spectral information of pixels grouped in segments given by the structure of the downsampling matrix $\boldsymbol{\Delta}$. It is important to note that, similar as in [17], in the following sections we assume that $K = N_{seg}$.

3. PROPOSED CSI CLUSTERING

Taking into account the sensing matrix construction approach presented in Eq. 2, it is possible to design the downsampling matrix $\boldsymbol{\Delta}$ to efficiently extract clustering features from the compressed measurements. In this section, we present an unsupervised approach to perform both, $\boldsymbol{\Delta}$ matrix design and clustering of the spectral image pixels by directly using the compressed measurements. The complete workflow of the proposed approach is depicted in Fig. 1.

3.1. Downsampling Matrix Design

In general, the matrix $\boldsymbol{\Delta} \in \mathbb{R}^{N_{seg}\times MN}$ groups the $M \times N$ spectral pixels in N_{seg} segments, such that each component of the vector $\bar{\mathbf{f}}_l = \boldsymbol{\Delta}\mathbf{f}_l$ contains the average spectral information of pixels grouped in one segment. More formally, denote $\mathbf{p}^e$ as the vector of size n_e containing the indices of all pixels belonging to the e-th segment. Then, the nonzero values of the $e - th$ row of $\boldsymbol{\Delta}$, denoted in vector form as $(\delta_e)^T$, are determined by the entries of $\mathbf{p}^e$ and the value of n_e as follows:

$$(\delta_e)^T_{(\mathbf{p}^e)_j} = \frac{1}{n_e}, \quad \text{for } j = 1, \cdots, n_e, \tag{5}$$

where $(\delta_e)^T_{(\mathbf{p}^e)_j}$ denotes the position in δ_e indexed by the $j - th$ entry of the vector $\mathbf{p}^e$.

The main idea of the proposed design of $\boldsymbol{\Delta}$ is to group pixels such that similar spectral information is taken into account. As only the compressed measurements are available and we do not have information from VIS spectrum (we are only interested in NIR), we propose to design $\boldsymbol{\Delta}$ in an iterative hierarchical fashion such that $Nseg$ increases (fewer pixels are grouped in one square (regular) segment) in each iteration.

At each iteration it, N_{seg} is selected as $N_{seg}^{(it)} > N_{seg}^{(it-1)} > \cdots > N_{seg}^{(1)}$ such as all the new segments are square and spatially homogeneous. Then, the $\mathbf{p}^e$ vectors are built for each segment e, and the new $\boldsymbol{\Delta}$ matrix is obtained using the Eq. 5 (see Algorithm 1). Once the compressed measurements are acquired, the feature vector $\bar{\mathbf{f}}_l$ is obtained for each spectral band l, hence the feature matrix $\bar{\mathbf{F}}$ is constructed as

$$\bar{\mathbf{F}} = \left[\bar{\mathbf{f}}_1, \cdots, \bar{\mathbf{f}}_L\right] \in \mathbb{R}^{N_{seg}\times L}, \tag{6}$$

where the rows contain the average spectral information of each segment.

3.2. Data Clustering

At each iteration of the main algorithm, the downsampling matrix $\boldsymbol{\Delta}$ is constructed, and it is used to obtain a partial clustering of the pixels using a subspace clustering method. Since,

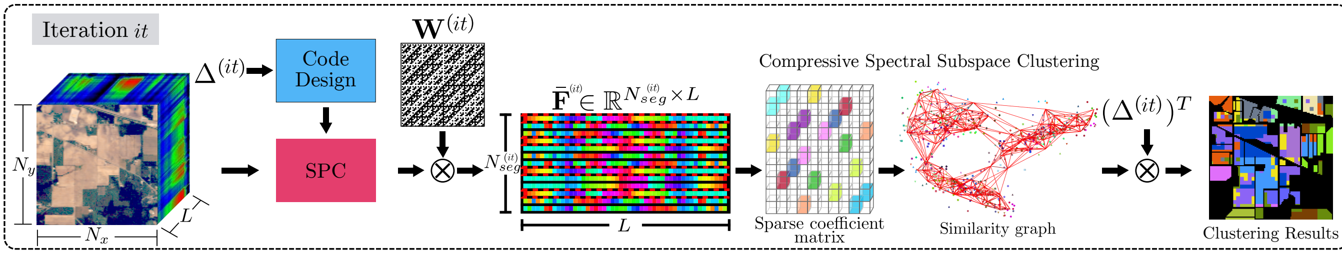

Fig. 1. Our Proposed SPC infrared clustering approach. For each iteration it in the hierarchy, we design the coded apertures using the decimation matrix $\mathbf{\Delta}^{(it)}$. With the designed codes, we acquire the compressed measurements with our SPC architecture (see Fig. 3). Then, we obtain the classification features using Eq. 4, which involves multiplying the SPC measurements with the Hadamard matrix $\mathbf{W}$. Finally, we apply compressive spectral subspace clustering to acquire the clustering map for the iteration it. After it iterations, the final segmentation map is obtained through the majority voting method in the partial clustering results at each hierarchy step.

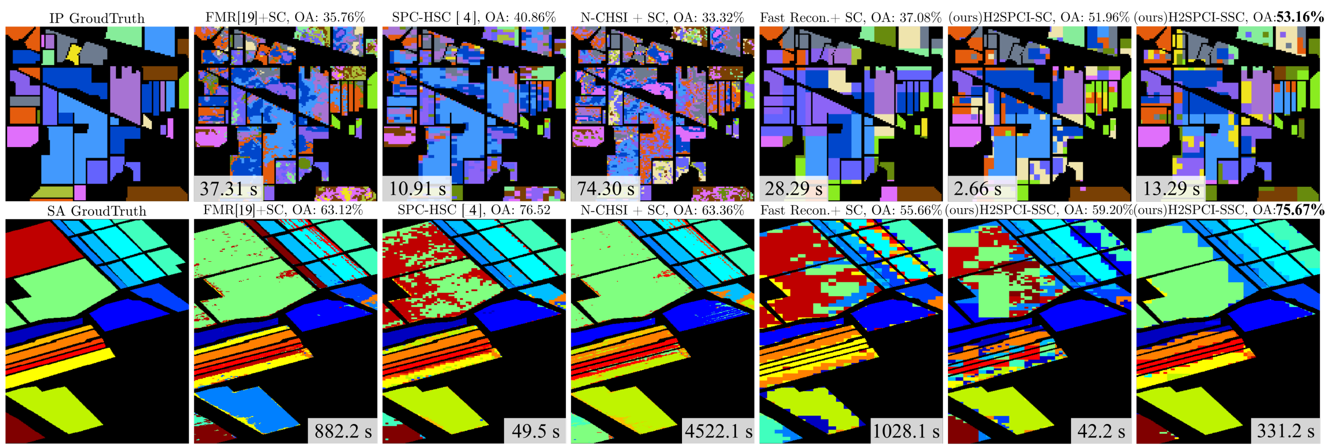

Fig. 2. Ground truth, visual and quantitative results (Overall Accuracy OA and Time in seconds) of different clustering approaches for the Indian Pines and Salinas Valley images. FMR[18]+SC and SPC-HSC [4] acquire SPC measurements from the near-infrared (NIR) and visible (VIS) spectrum, while the others only use the information from the NIR.

at each iteration it, the number of segments N_{seg} is increased, this approach can be seen as a multi-scale clustering of pixels. Furthermore, denoting N_s as the number of scales or levels in the hierarchy, the compression ratio given by using the SPC architecture and the proposed clustering approach can be determined as

$$\tilde{\gamma} = \frac{1}{MN} \sum_{it=1}^{N_s} N_{seg}^{(it)}. \tag{7}$$

In order to perform spectral clustering [19], we construct a similarity graph $\mathbf{G} \in \mathbb{R}^{MN \times MN}$ using the κ-nearest neighbor approach described in [19]. Then, the cluster indices $\bar{\mathbf{C}}$ are obtained by applying the spectral clustering to the similarity graph. Finally, the cluster membership of all the spectral pixels in the full image are obtained by applying the upsampling operator $\mathbf{\Delta}^T$ onto $\bar{\mathbf{C}}$, see Algorithm 2. Note that both, the similarity graph construction and the spectral clustering computation are performed on the feature matrix $\bar{\mathbf{F}}$. Hence, the computational performance of the proposed method improves over other traditional approaches.

4. RESULTS

4.1. Simulations

In this section, the proposed hierarchical compressed subspace clustering method for SPC measurements is tested on two real remote sensing hyperspectral datasets: Indian pines and Salinas. The ground truth of these datasets contains 16 land-cover classes. In this work, we use a region of interest (ROI) from the **Indian Pines** image of 512×217 pixels and 200 spectral bands [20]. From the **Salinas Valley** image, we use a ROI of 512×192 spatial pixels, and 204 spectral bands in the range of 240 to 2400 nm.

Figure 2 presents the ground truth, clustering visual and numerical results on the two spectral datasets with four methods of the literature and our proposed approach with two subspace clustering methods: spectral clustering[19] and sparse subspace clustering [21]. Each row contains a different dataset and each column is defined as follows: The first column presents the ground truth. The second, which we

Algorithm 1 Downsampling Matrix Design

Require: N_{seg}, $\bar{\mathbf{F}}$
Ensure: $\mathbf{\Delta}$
procedure DSAMPLING_DESIGN($\bar{\mathbf{F}}, N_{seg}$)
  $k_{idx} \leftarrow$ RegularSegms($\bar{\mathbf{F}}, N_{seg}$) ▷ k_{idx} contains the segment labels
  $\mathbf{\Delta} \leftarrow$ zeros(N_{seg}, length(k_{idx}))
  for $e \leftarrow 1$ to N_{seg} **do**
    $\mathbf{p}^e \leftarrow$ find($k_{idx} = e$)
    $n_e \leftarrow$ length($\mathbf{p}^e$)
    for $j \leftarrow 1$ to n_e **do**
      $(\delta_e)^T_{(\mathbf{p}^e)_j} = \frac{1}{n_e}$ ▷ Update each row of $\mathbf{\Delta}$
    end for
  end for
  return $\mathbf{\Delta}$
end procedure

Algorithm 2 Data Clustering

Require: $\bar{\mathbf{F}} \in \mathbb{R}^{N_{seg} \times L}$, $\mathbf{\Delta}$ downsampling matrix, κ clusters
Ensure: Segmentation of the spectral pixels: $\mathbf{F}_1, \cdots, \mathbf{F}_k$
procedure DATA_CLUSTERING($\bar{\mathbf{F}}, \mathbf{\Delta}, \kappa$)
  $\mathbf{G} \leftarrow$ Build_Sim_Graph($\bar{\mathbf{F}}$) ▷ κ-nearest neighbor graph ▷ Obtain Cluster indices
  $\bar{\mathbf{C}}_{idx} \leftarrow$ Spectral_Clustering($\mathbf{G}, \kappa$) ▷ Spectral Clustering [19]
  $\mathbf{C}_{idx} \leftarrow \mathbf{\Delta}^T \bar{\mathbf{C}}_{idx}$ ▷ Upsampling
end procedure

refer to as "FMR+SC", corresponds to the method described in [18], where δ is designed using super-pixels obtained from an RGB image which was acquired as side information. The third column, "SPC-HSC", exposes the results using the method proposed by authors in [4]. The fourth column shows the results when directly clustering the full (non-compressed) hyperspectral image. The fifth column presents the results of clustering the reconstructed SI obtained via the fast reconstruction method shown in Eq. 3. Finally, the two last columns correspond to clustering results obtained with the proposed method. All methods use the spectral clustering ("SC") algorithm [19], except our method shown in last column which use sparse subspace clustering ("SSC") [21]. It is important to highlight that the two first methods acquire SPC measurements from the visible (VIS) and near-infrared (NIR) spectrum, while the others four methods (including our proposed one) only use the information from the NIR. Numerical results of the evaluated methods are presented in Figure2, we shown the overall accuracy (OA) obtained by each method at the top. Also, Notice that for the Indian Pines dataset, the best OA is achieved by the proposed strategy in this paper, using the "SSC" algorithm. On the other hand, for the Salinas dataset, the best OA result is provided by the "SPC-HSC" method, and the second-best OA results are achieved by the proposed method with the "SSC" algorithm. However, considering that the "SPC-HSC" method uses the near-infrared (NIR) and visible (VIS) spectrum, our method suggests a competitive alternative that does not require visible spectrum information.

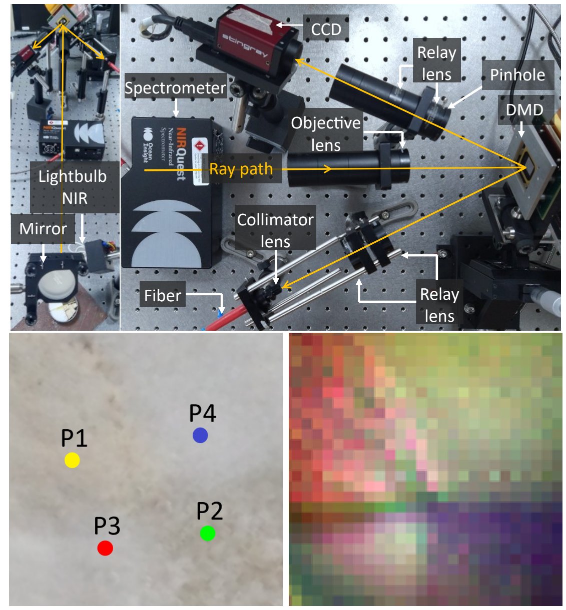

Fig. 3. Single-pixel imaging of a hyperspectral "White" scene. (a) Sketch of the experimental setup. (b) RGB composite acquired with a commercial camera. (c) False RGB composite obtained via Eq. (3) with $N_{seg} = 64$.

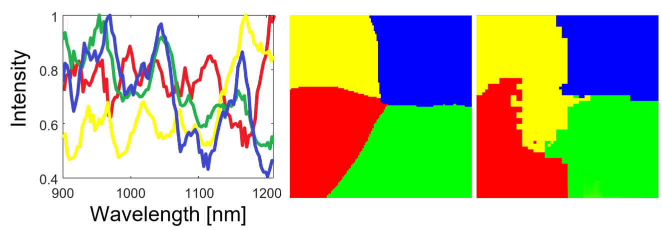

Fig. 4. (Left) Average spectral signature for each class. (Middle) Ground truth. (Right) Classification result via majority voting with $OA = 85\%$.

4.2. Experiments

We built a testbed in our laboratory to demonstrate the validity of the proposed ideas, through a proof-of-concept prototype, as shown in Fig. 3 (a). This prototype uses an uncoated N-BK7 Bi-Convex lens (Lens 1) (Thorlabs LB1676-ML, $f1 = 100.0mm$) as an objective lens to propagate the incoming wavefront to image the scene onto the digital micromirror device (DMD, Texas Instruments, D4120). The DMD introduced a spatial modulation, and the resulting coded wavefront propagates through two uncoated N-BK7 Bi-Convex lenses (Lens 2-3) (Thorlabs LB1676-ML, $f1 = 100.0mm$) located in sequence to reduce the wavefront propagation distance.

This coupled lens generated imaging over the surface of a collimator lens (Ocean Insight, 74-UV with wavelength range 185nm - 2500nm) coupled to an optical fiber (Ocean Insight, QP1000-2-VIS-BX, with fiber core size 1000 μm). This fiber transmits the collimated-modulated wavefront to a NIR-spectrometer (Ocean Insight, NIRQUEST+2.5 Spectrometer with entrance slit 25 μm), which decomposes the incoming wavefront into 512 spectral values in the wavelength range 900nm - 2500nm, i.e., 512 pixels are captured for each 128×128 DMD pattern (each encoding pixel occupied 2×2 DMD pixels). Here, the auxiliary grayscale camera is used for calibration and monitoring purposes.

To demonstrate the proposed methodology classification capability, we conducted experimental validations using one composed target (named "White" scene), as shown in Fig. 3 (b)-(c). This target is composed of four white materials: (P1) milk powder, (P2) sugar, (P3) bicarbonate, and (P4) salt. Using this scene, we aim to explicitly show the importance of considering the NIR for classification as pixels of this scene are very challenging to discriminate using only the information from the visible spectrum (VIS). For five hierarchical iterations with $N_{seg} = \{4^2, 8^2, 16^2, 32^2, 64^2\}$ the resulting compressive measurement exhibited $512 \times N_{seg}$ spectrometer pixels in size. The coded apertures patterns projected by the DMD were generated via Eq. (2) with a Hadamard matrix size of $\mathbf{W} \in \mathbb{R}^{MN \times MN}$ and $\mathbf{H} \in \mathbb{R}^{N_{seg} \times MN}$ where $M = N = 128$. Since the resulting matrix $\mathbf{H}$ is composed of $\{-1, 0, 1\}$ values and it is not feasible to load negative values in the DMD [18], the sensing process is carried out by changing the -1's values for 0's. Then resulting binary pattern and a complementary version (i.e., changing 1's to 0's and 0's to 1's) of it are projected on the DMD. Finally, the acquired two measurements per pattern are reduced to $y_{10} - y_{01}$ in post-processing, i.e., y_{10} and y_{01} refers to the SPC measurement obtained from the binary and complementary versions.

Figure 4 shows (left) the average spectral signature of each class, (middle) the ground truth map, and (right) the corresponding clustering map obtained by our method when using the "White" scene as input. These results were achieved by exploiting the NIR information preserved in the compressed measurements. To support the classification results shown in 4 (b), one representative spectral signature for each material is plotted in Fig. 4 (c). These four signatures were recovered directly from the compressed measurement via Eq. (3). To further analyze the hierarchical classification performance, Fig. 5 shows each individual clustering results for $N_{seg} = \{4^2, 8^2, 16^2, 32^2, 64^2\}$, where we achieve an OA of 81%, 65%, 83%, 82%, and 79%, respectively for each N_{seg}. The higher classification accuracy was achieved for $N_{seg} = 16^2$ (i.e., each segments have a size of 8×8), and the lower one was achieved for $N_{seg} = 64^2$ (i.e., each segment have a size of 2×2). Since the pattern's pixel size proportionally increases with the regular decimation pixel size (as shown in Fig. 5 middle row), the acquired SPC measurements

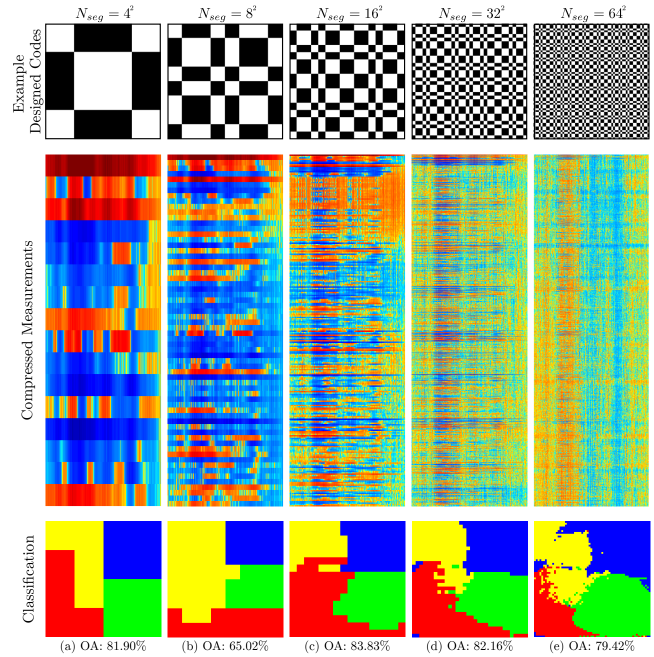

Fig. 5. (first row) Coded aperture structure for an arbitrary number of segments. (second row) Raw compressed single-pixel measurement. (third row) Individual classification results for five different decimation levels.

are more robust to noise artifacts (see Fig. 5 bottom row), a critical consideration in infrared experiments. Here the classification accuracy obtained using $N_{seg} = 8^2$ is deliberately set aside because it is assumed as an outlier.

5. CONCLUSIONS

This work presented a sensing matrix designed to extract features directly from the compressed measurements in each stage of the hierarchical model. We demonstrate that the proposed imaging system, together with the sensing protocol and the computational algorithm, represents an efficient alternative to estimate clustering maps without relying on oversampling sensing protocols. This paper showed extensive results on simulations and experimental proof-of-concept implementation. These results demonstrated that creating the final segmentation map through the majority voting method in the partial clustering results at each hierarchy step with the sensing matrices designed, achieves competitive results against other state-of-the-art methods. The main contribution presented in this document is the alternative to spectral clustering in CSI measurements only using the NIR spectrum and excluding the information from the traditional visible range.

Acknowledgement

This work was supported by the "Sistema General de Regalías Colombia" (BPIN 2020000100415, with UIS code 8933).

6. REFERENCES

[1] Karen Sanchez, Carlos Hinojosa, and Henry Arguello, "Supervised spatio-spectral classification of fused images using superpixels," *Applied optics*, vol. 58, no. 7, pp. B9–B18, 2019.

[2] Jorge L Bacca, Carlos A Hinojosa Montero, and Henry Arguello, "Kernel sparse subspace clustering with total variation denoising for hyperspectral remote sensing images," in *Mathematics in Imaging*. Optical Society of America, 2017, pp. MTu4C–5.

[3] Carlos A Hinojosa, Fernando Rojas, Sergio Castillo, and Henry Arguello, "Hyperspectral image segmentation using 3d regularized subspace clustering model," *Journal of Applied Remote Sensing*, vol. 15, no. 1, pp. 016508, 2021.

[4] Carlos Hinojosa, Jorge Bacca, Edwin Vargas, Sergio Castillo, and Henry Arguello, "Single-pixel camera sensing matrix design for hierarchical compressed spectral clustering," in *2019 IEEE MLSP*. IEEE, 2019.

[5] Jhon Lopez, Carlos A Hinojosa, and Henry Arguello, "Efficient subspace clustering of hyperspectral images using similarity-constrained sampling," *Journal of Applied Remote Sensing*, vol. 15, no. 3, pp. 036507, 2021.

[6] Mathieu Fauvel, Yuliya Tarabalka, Jon Atli Benediktsson, Jocelyn Chanussot, and James C Tilton, "Advances in spectral-spatial classification of hyperspectral images," *Proceedings of the IEEE*, vol. 101, no. 3, pp. 652–675, 2012.

[7] Jonathan Monsalve, Juan Ramirez, Iñaki Esnaola, and Henry Arguello, "Covariance Estimation from Compressive Data Partitions using a Projected Gradient-based Algorithm," *arXiv:2101.04027*, jan 2022.

[8] Jonathan Monsalve, Miguel Marquez, Iñaki Esnaola, and Henry Arguello, "Compressive covariance matrix estimation from a dual-dispersive coded aperture spectral imager," in *2021 IEEE International Conference on Image Processing (ICIP)*. IEEE, 2021, pp. 2823–2827.

[9] Claudia V Correa, Carlos Hinojosa, Gonzalo R Arce, and Henry Arguello, "Multiple snapshot colored compressive spectral imager," *Optical Engineering*, vol. 56, no. 4, pp. 041309, 2016.

[10] Amir Beck and Marc Teboulle, "A fast iterative shrinkage-thresholding algorithm for linear inverse problems," *SIAM journal on imaging sciences*, vol. 2, no. 1, pp. 183–202, 2009.

[11] Mário AT Figueiredo, Robert D Nowak, and Stephen J Wright, "Gradient projection for sparse reconstruction: Application to compressed sensing and other inverse problems," *IEEE Journal of selected topics in signal processing*, vol. 1, no. 4, pp. 586–597, 2007.

[12] Joel A Tropp and Anna C Gilbert, "Signal recovery from random measurements via orthogonal matching pursuit," *IEEE Transactions on information theory*, vol. 53, no. 12, pp. 4655–4666, 2007.

[13] Kevin Arias, Edwin Vargas, and Henry Arguello, "Hyperspectral and multispectral image fusion based on a non-locally centralized sparse model and adaptive spatial-spectral dictionaries," in *2019 27th European Signal Processing Conference (EUSIPCO)*. IEEE, 2019.

[14] Carlos Hinojosa, Karen Sanchez, Hans Garcia, and Henry Arguello, "C-3SPCD: coded aperture similarity constrained design for spatio-spectral classification of single-pixel measurements," *Applied Optics*, vol. 61, no. 8, pp. E21–E32, 2022.

[15] Marco F Duarte, Mark A Davenport, Dharmpal Takhar, Jason N Laska, Ting Sun, Kevin F Kelly, and Richard G Baraniuk, "Single-pixel imaging via compressive sampling," *IEEE signal processing magazine*, vol. 25, no. 2, pp. 83–91, 2008.

[16] Aswin C Sankaranarayanan, Lina Xu, Christoph Studer, Yun Li, Kevin F Kelly, and Richard G Baraniuk, "Video compressive sensing for spatial multiplexing cameras using motion-flow models," *SIAM Journal on Imaging Sciences*, vol. 8, no. 3, pp. 1489–1518, 2015.

[17] H. Garcia, C. V. Correa, and H. Arguello, "Multi-resolution compressive spectral imaging reconstruction from single pixel measurements," *IEEE Transactions on Image Processing*, vol. 27, no. 12, pp. 6174–6184, Dec 2018.

[18] Hans Garcia, Claudia V Correa, Karen Sánchez, Edwin Vargas, and Henry Arguello, "Multi-resolution coded apertures based on side information for single pixel spectral reconstruction," in *2018 26th European Signal Processing Conference (EUSIPCO)*. IEEE, 2018, pp. 2215–2219.

[19] Ulrike Von Luxburg, "A tutorial on spectral clustering," *Statistics and computing*, vol. 17, no. 4, 2007.

[20] Hongyan Zhang, Han Zhai, Liangpei Zhang, and Pingxiang Li, "Spectral–spatial sparse subspace clustering for hyperspectral remote sensing images," *IEEE Transactions on Geoscience and Remote Sensing*, vol. 54, no. 6, pp. 3672–3684, 2016.

[21] Ehsan Elhamifar and René Vidal, "Sparse subspace clustering: Algorithm, theory, and applications," *IEEE transactions on pattern analysis and machine intelligence*, vol. 35, no. 11, pp. 2765–2781, 2013.